ELSEVIER

Contents lists available at ScienceDirect

## Journal of Inorganic Biochemistry

journal homepage: www.elsevier.com/locate/jinorgbio





# Comparative study of the binding and activation of 2,4-dichlorophenol by dehaloperoxidase A and B

Mst Sharmin Aktar, Vesna de Serrano, Reza Ghiladi, Stefan Franzen

Department of Chemistry, North Carolina State University, Raleigh, NC 27695, United States of America

ARTICLE INFO

Keywords:
Peroxidase
2,4-dichlorophenol
electron transfer
Activation energy
Enzyme kinetics
Solvent effect

#### ABSTRACT

The dehaloperoxidase-hemoglobin (DHP), first isolated from the coelom of a marine terebellid polychaete, Amphitrite ornata, is an example of a multi-functional heme enzyme. Long known for its reversible oxygen (O2) binding, further studies have established DHP activity as a peroxidase, oxidase, oxygenase, and peroxygenase. The specific reactivity depends on substrate binding at various internal and external binding sites. This study focuses on comparison of the binding and reactivity of the substrate 2,4-dichlorophenol (DCP) in the isoforms DHPA and B. There is strong interest in the degradation of DCP because of its wide use in the chemical industry, presence in waste streams, and particular reactivity to form dioxins, some of the most toxic compounds known. The catalytic efficiency is 3.5 times higher for DCP oxidation in DHPB than DHPA by a peroxidase mechanism. However, DHPA and B both show self-inhibition even at modest concentrations of DCP. This phenomenon is analogous to the self-inhibition of 2,4,6-trichlorophenol (TCP) at higher concentration. The activation energies of the electron transfer steps in DCP in DHPA and DHPB are  $19.3 \pm 2.5$  and  $24.3 \pm 3.2$  kJ/mol, respectively, compared to  $37.2 \pm 6.5$  kJ/mol in horseradish peroxidase (HRP), which may be a result of the more facile electron transfer of an internally bound substrate in DHPA. The x-ray crystal structure of DHPA bound with DCP determined at 1.48 Å resolution, shows tight substrate binding inside the heme pocket of DHPA (PDB 8EJN). This research contributes to the studies of DHP as a naturally occurring bioremediation enzyme capable of oxidizing a wide range of environmental pollutants.

#### 1. Introduction

Dichlorophenols have a wide range of applications as intermediates in the synthesis of pesticides and herbicides, but also are present in waste streams from the pulp and paper industry [1]. Some dichlorophenols are used as disinfectants and preservatives in personal care and cosmetic products. However, excessive exposure to dichlorophenols can lead to a number of health and environmental problems [2]. Moreover, dichlorophenol is considered as a pollutant by the Environmental Protection Agency (EPA) in the United States because it can result from the chlorination of drinking water and is found in wood preservatives [3]. There are two main types of dichlorophenol: 2,4-dichlorophenol (2,4-DCP) and 2,6-dichlorophenol (2,6-DCP) and both of them are classified as priority pollutants by the EPA and known to cause adverse health effects and are monitored in drinking water and other environmental samples [4-6]. We will focus on 2,4-DCP, which is called DCP in the remainder of the study. DCP is also a precursor to the formation of dioxins which are among the most toxic compounds known. For example,

in the marine environment polybrominated dibenzo-p-dioxins (PBDDs) have been isolated from an aquatic sponge *Ephydatia fluviatilis* [7,8].

Oxidative dehalogenation of trihalophenols into their corresponding dihaloquinones is a well-known reaction catalyzed by peroxidase enzymes [9]. In the peroxidase reaction cycle, following activation by hydrogen peroxide bound to a heme, two sequential electron transfers lead to formation of neutral phenoxy radicals. These radicals disproportionate to form one equivalent of substrate and one equivalent of a phenoxy cation, which reacts to form a quinone by incorporation of oxygen from a water molecule and loss of a hydrohalide. However, radicals can also initiate polymerization initiated by reaction of the phenolate radical with a C-H bond of a neutral phenol. The carbons in the ortho and para positions are most reactive. For a given substrate the polymer yield depends on whether the binding occurs externally as in HRP or internally as observed in DHP. We anticipate that the polymerization yield will be much greater for DCP than for TCP in HRP because of the chlorine atoms in both ortho positions of the latter. Previous studies have shown that DCP binds internally in the distal pocket of

E-mail address: franzen@ncsu.edu (S. Franzen).

<sup>\*</sup> Corresponding author.

DHPB which may reduce the polymerization yield [10]. This is one hypothesis to be tested by comparing the reactivity and structure of DCP binding in to the two different isoforms of DHP.

The name DHP refers to dehalogenation via a peroxidase mechanism. DHP is found in the coelom of a marine terebellid polychaete Amphitrite ornata. DHP functions as a monomeric hemoglobin for transporting oxygen [11,12]. It was first discovered as a hemoglobin in 1977 [13] and later it is rediscovered as an enzyme with peroxidase function in 1996 [9]. In the earliest quantitative comparison, the peroxidase activity of DHPA was measured in aqueous buffer at pH 7 and found to be 12 times higher than myoglobin and 13 times lower than HRP [14]. Subsequent studies have revealed a range of functions, including peroxygenase, oxygenase, and oxidase, each related to the specific structure of a class of substrates that bind in or on DHP [15-17]. Different species of marine worms in the hemichordate family such as Saccoglossus kowalevskii and the polychaete family Notomastus lobastus co-habit benthic ecosystems with Amphitrite ornata. A benthic ecosystem refers to a marine seabed, typically with mud rather than sand bottom. Many worms, including the ones mentioned above, synthesize and sometimes secrete toxic halogenated metabolites such as bromophenols, bromoindoles, bromopyrroles

as part of their defense against predators [9]. Amphitrite ornata is a tube worm and is therefore immobile. A. ornata is believed to survive in this toxic environment by using the enzyme DHP to oxidize and dehalogenate brominated aromatic compounds in the benthic ecosystem. The general dehalogenation mechanism of phenolic substrate involves proton-coupled electron transfer from the substrate to the enzyme, leading to a formation of an intermediate radical which undergoes disproportionation to form a haloguinone with loss of one halogen substituent from the ring. Substrates have various internal binding sites that depend on their structure. These have been classified by comparing crystal structures of bound substrates with the  $\alpha$ -,  $\beta$ -,  $\gamma$ -, and  $\delta$ -edges of the heme. The  $\beta$ -binding site is inhibitory, while that  $\alpha$ - and  $\gamma$ -binding sites promote peroxidase and peroxygenase function, respectively, with the possible occurrence of self-inhibition at high substrate concentration [18-24]. The heme structure and definition of the edges relevant to these descriptions are shown in Fig. S1 in the Supporting Information.

Fig. 1. Proposed peroxidase mechanism for DHP-catalyzed oxidation of dihalophenols.

# 1.1. Peroxidase kinetic theory: substrate oxidation via heme activation and electron transfer

Fig. 1 shows the reaction cycle. The distal histidine in DHP, H55, catalyzes the first step in the peroxidase mechanism of DHP which is the reduction of  $\rm H_2O_2$  to  $\rm H_2O$  by cleavage of the O—O bond. This process converts ferric DHP to compound I, an oxo intermediate with a porphyrin  $\pi$ -cation radical. This cation radical can be transferred to an adjacent amino acid (Y34 for DHPA and Y38 for DHPB) [25] through internal electron transfer and a new species, called compound ES, is formed. Compound ES can oxidize 2,4-dihalophenol into its phenoxy radical, forming compound II, an Fe oxo intermediate with a neutral heme. Compound II can oxidize a second substrate molecule, which returns DHP to its ferric resting state.

The rate constant for the activation step, k1, has been characterized by the Poulos-Kraut mechanism showing a rearrangement of Fe-O(H)OH to Fe-O-OH<sub>2</sub> followed by rupture of the O—O bond. The role of the heme and protein is characterized by the push-pull mechanism, which refers to strong ligation of the Fe to support high oxidation states of the ferryl intermediate and a role by distal amino acids to extracted (H) and replace it on the more distal O atom. The activation of H<sub>2</sub>O<sub>2</sub> is not shown explicitly in Fig. 1, which shows the two one-electron oxidation steps that complete the enzymatic cycle in the presence of  $H_2O_2$  [9,26,27]. The peroxidase mechanism has historically been observed as an external substrate binding followed by electron transfer [28]. However, substrates can bind in various locations near the y-edge of the heme [71-73]. DHP crystal structures have shown three internal substrate binding sites in the distal pocket of the globin. The  $\alpha$ -site deep in the protein may facilitate two-step peroxidase chemistry in situ. The  $\beta$ -site is known as an inhibitor site and the  $\gamma$ -sites in DHP may permit peroxygenase or peroxidase mechanisms. There are conformations that do not conform to any of these three main modes of binding.

Fig. 2 shows the oxidative dehalogenation of 2,4,6-trichlorophenol (TCP) to 2,6-dichloro-1,4-benzoquinone (DCQ) and of 2,4-dichlorophenol (DCP) to 2-chloro-1,4-benzoquinone (2-ClQ). The brominated analog, 2,4-dibromophenol is a naturally occurring xenobiotic that is significantly more prevalent in marine ecosystems than 2,4,6-tribromophenol (TBP). Despite its relatively low prevalence in the environment, TBP has been studied as substrate due to its high toxicity. TCP is a more soluble analog of TBP that has been widely studied as well. On the other hand, DHP activity toward DCPB has been studied relatively recently [10].

Fig. 2 also shows that the major product of hydrogen peroxide  $(H_2O_2)/DHP$  catalyzed oxidation reaction of 2,4-dichlorophenol (DCP) is 2-chloro-1,4-benzoquinone (2-ClQ). Malewschik and coworkers concluded that DHPB catalyzes oxidation of DCP by two different mechanisms namely oxidation and oxidative dehalogenation [10]. Initial substrate oxidation follows peroxidase activity and the subsequent oxidation via hydroxylation by  $H_2O_2$ . In addition to this major pathway, Malewschik also reported direct oxidation of DCP to a catechol product, via a peroxygenase mechanism. The peroxygenase mechanism also involves formation of compound I followed by O-atom transfer to the substrate, usually to insert between a C—H bond [17]. The peroxygenase mechanism requires internal binding of the substrate to facilitate O-atom transfer [17].

HRP is also known to oxidize DCP and other dihalogenated phenols

to form the quinones accompanied by significant polymerization [6,29–32]. HRP binds substrates at an external site on the  $\delta$ -edge of the heme [28], while DHP binds DCP at a site inside the distal pocket of the globin. Internal binding of DCP reduces the extent of polymerization, which is important for biological function given that DHP is found in the coelom of *A. ornata*. DHP appears to facilitate peroxidase chemistry via two sequential electron transfers from substrates bound in the distal pocket, thus minimizing the polymerization side reaction. Polymerization of halogenated phenols is a principal goal of HRP studies for the purpose of remediation of polluted water [33,34]. Kinetics is less complex for TCP, which has a lower polymerization yield. TCP has used a model of peroxidase kinetics.

A complete analysis of the rate scheme in Fig. 1 is presented in the Supporting Information section S.2. The kinetic analysis permits measurement of the proton-coupled electron transfer rate constants,  $k_2$  and  $k_3$ , from substrate to heme iron in the ferryl heme radical (Cmpd I) and ferryl neutral heme (Cmpd II) forms. Electron transfer  $k_3$  is the rate limiting step in the peroxidase reaction cycle. Measurements show that  $k_3$  is between 10 and 20 times smaller than  $k_2$  [35]. For sake of a consistent comparison, it is assumed here that  $k_3$  is 10 times slower than  $k_2$ . The comparison of Michaelis-Menten and peroxidase rates schemes shows that  $k_2$  and  $k_3$  are related to  $k_{cat}$ /  $K_M$ . Using the approximations given in the Supporting Information (Eq. S15) we can obtain the value of  $k_2$ .

$$\frac{k_{cat}}{K_M} = \frac{k_2}{5.5} \tag{1}$$

The linear portion of the Michaelis-Menten saturation plot, shown in Fig. S2, which has a slope of  $k_{cat}/K_M$  at low substrate concentration, [S]  $< K_M$ . Eq. 1 shows that even for limited substrate concentrations the linear region of the peroxidase saturation plot provides information on the electron transfer rate constants from substrate to heme iron. The kinetic plots are nearly linear for HRP and  $K_M$  is large and the saturation region is not observed. Since DHPA and B have slower rates, the saturation region is observed and one can obtain separate estimates for  $k_{cat}$  and  $k_M$ , permitting all three peroxidase rate constants to be obtained. However, the electron transfer rate constants,  $k_2$  and  $k_3$ , are of the greatest interest for comparison of substrate binding and reactivity.

From an Arrhenius plot of the temperature dependence of  $k_2$  and  $k_3$ we measured the activation energy, which can be interpreted in terms of Marcus theory as described in the Supporting Information section S.3 and shown in Eq. S18. While the reorganization energy cannot be directly measured, it can be obtained from the activation energy, measured from an Arrhenius plot, and the driving force, measured previously by electrochemistry and pulse radiolysis [35-39]. The reorganization energy provides information relevant to the solvent environment of the substrate. Therefore, the experiments in this study address the issue of the role of internal binding of substrates in DHP compared to the known external binding in HRP. The high-bindingaffinity internal mode of binding of DCP in both isoforms of DHP suggests that self-inhibition is important. The role of a molecule as substrate or inhibitor depends on the mode of binding in the distal pocket. To address this issue, we have determined the x-ray crystal structures of bound substrate and compared DCP binding in the two isoforms of DHP.

$$X \rightarrow CI$$
+  $H_2O_2$ 

DHP/HRP

 $X \rightarrow CI$ 
+  $H_2O$  +  $HCI$ 

Fig. 2. Peroxidase reactions of halophenols catalyzed by DHP. When X = H, the DCP oxidation yields 2-chloro-1,4-benzoquinone and when X = Cl, TCP oxidation affords 2,6-dichloro-1,4-benzoquinone.

#### 2. Experimental

#### 2.1. Materials and methods

All chemicals were purchased from Sigma-Aldrich, Acros, VWR or Fisher Scientific and used without further purification. Acetonitrile (ACN) and trifluoroacetic acid (TFA) were HPLC grade. Wild-Type (WT) Histidine-Tagged (His6X) DHPA and DHPB were expressed and purified following the previously described procedure [19,20]. The protein was oxidized, to obtain the ferric state, before each kinetics, HPLC or LC-MS experiment by adding an excess of potassium ferricyanide, K<sub>3</sub>[Fe(CN)<sub>6</sub>] and passing the solution through a PD-10/sephadex G-25 desalting column [21] to remove the excess K<sub>3</sub>[Fe(CN)<sub>6</sub>]. Horseradish peroxidase (HRP) ( $\varepsilon_{403} = 102,000 \text{ M}^{-1} \text{ cm}^{-1}$ ) [24] was procured from MilliporeSigma and used as received. Stock solutions of the substrates: 2,4,6trichlorophenol (TCP), 2,4-dichlorophenol (DCP), were prepared in 100% methanol (MeOH) stock solutions and stored in a - 80 °C freezer until needed. The percentage of methanol in the final sample was 5% in all experiments where MeOH was a cosolvent. A stock solution of hydrogen peroxide ( $H_2O_2$ ) ( $\varepsilon_{240} = 43.6 \text{ M}^{-1} \text{ cm}^{-1}$ ) was freshly prepared using 30% reagent grade hydrogen peroxide in 100 mM KPi buffer of corresponding pH (7 µL of H<sub>2</sub>O<sub>2</sub> in 10 mL of buffer) before each experiment and kept on ice before using. The concentration of DHP, HRP, H<sub>2</sub>O<sub>2</sub> were determined spectrophotometrically using extinction coefficient  $\varepsilon_{406} = 116,400 \text{ M}^{-1} \text{ cm}^{-1}, \varepsilon_{403} = 102,000 \text{ M}^{-1} \text{ cm}^{-1}$  and  $\varepsilon_{240}$ = 43.6 M<sup>-1</sup> cm<sup>-1</sup> respectively [20]. Catalase (MP Biomedicals, LLC, Solon, OH) was used to quench the reaction mixer in HPLC experiments. Catalase was stored at 4 °C until needed. Stock solutions of 3.5 M ammonium sulfate, sodium cacodylate (pH 6.5) and different grades of PEG (2000, 4000, 5000 and 8000), crystal setting well plates, cryoloops, crystal caps, cover slips and all the solutions used for crystallization experiments were purchased from Hampton Research, California.

#### 2.2. Temperature dependent UV-visible kinetic assay with DCP and TCP

The temperature-controlled kinetic reactions were performed in triplicate for DHPA, DHPB and HRP with both substrates (DCP and TCP), using the kinetic mode in a UV-Visible spectrophotometer; Agilent Cary 3500 UV-Vis Compact Peltier spectrophotometer (Mulgrave, Australia). The analysis was performed using Cary UV Workstation software. The reactions were carried out at four different temperatures: 10 °C, 15 °C, 20 °C, and 25 °C. Experiments were also attempted at 30 °C but had low vields and a significant decrease in rate, which we attributed to denaturation of the protein due to the combination of temperature and the use of 5% methanol in the solution and were not further pursued. The instrument was set to the target temperature and each sample was allowed to equilibrate for 3 min prior to each experiment. All the kinetic reactions were carried out in a quartz cuvette of 0.4 cm pathlength from Starna Cells (Atascadero, California), keeping the total sample volume 1 mL in 5% MeOH solution. The final concentration of the enzymes was kept constant, 2.4  $\mu$ M for both DHPA and DHPB and 60 nM for HRP. The substrate concentration for DCP varied between 0.03 and 1.5 mM and for TCP 0.05-1.5 mM. Initially enzyme and substrate were mixed together and subsequently, the reaction was initiated by adding freshly prepared  $H_2O_2$  at a constant concentration of 1200  $\mu M$ . The product formation, 2-ClQ for the DCP reaction and 2,6-DCQ for the TCP reaction were monitored at 255 nm ( $\epsilon_{255} = 16,900 \text{ M}^{-1} \text{ cm}^{-1}$ ) [22] and 273 nm  $(\varepsilon_{273} = 13,200 \text{ M}^{-1} \text{ cm}^{-1})$  [23], respectively. Kinetic experiments were monitored for 90 s with spectral measurements over a range from 220 to 320 nm taken every 2.5 s at pH 7. The wavelength range was selected to permit the observation of both the formation of quinone products, including hydroxylated quinones and consumption of substrates DCP and TCP.

#### 2.3. HPLC reactivity studies

Reversed-Phase HPLC was used to identify the reactivity, percent conversion of substrate into products, identification of product/products from the oxidation of DCP and/or TCP catalyzed by DHPs and HRP reactions at different pHs (pH 5,6,7 and 8). The instrument was comprised of a Waters e2695 bioseparations module with a Waters 2998 photodiode array detector provided with a Thermo-Scientific ODS Hyeprsil, particle size 5um (150 × 4.6 mm) C-18 column. A binary [Aqueous (A) and Organic (B)] solvent system was used to perform the separation of analytes (solvent A: water+0.1% TFA and solvent B: ACN+ 0.1% TFA) as mobile phase. Separation was carried out by a linear gradient of solvent A and B at a flow rate of 1.5 mL/min and the elution condition was as follows: 95:5 (A:B) to 5:95 linearly for 12 min; 5:95 isocratic for 2 min: 5:95 to 95:5 isocratic over 1 min and then isocratic for 3 min. The Empower 3 software package (Waters Corp., Massachusetts) was used to analyze the data. Enzyme assay reactions were performed in triplicate in 100 mM KPi buffer (pH 7 unless otherwise mentioned) at 25 °C with the final sample volume of 250 µL containing 5% MeOH. Substrate stock solutions of 10 mM were prepared in MeOH. Initially DHP (10  $\mu$ M) and substrate (500 µM) were mixed, and reaction was started by adding  $H_2O_2$  (500  $\mu$ M). The reaction was quenched after 5 mins (unless stated otherwise) with 5  $\mu$ L of catalase. Subsequently, the reaction mixture was diluted 4-fold with 100 mM KPi at the corresponding pH in order to determine the extent of substrate conversion. Control experiments were performed in absence of either H<sub>2</sub>O<sub>2</sub> (non-oxidant control) or enzyme (non-enzymatic control).

# 2.4. Product identification by liquid chromatography-mass spectrometry (LC-MS)

Analysis of undiluted samples (2  $\mu$ L injection volume) was carried out on a high-resolution mass spectrometer – the Thermo Fisher Scientific Exactive Plus MS, a benchtop full-scan Orbitrap mass spectrometer using Heated Electrospray Ionization (HESI). Samples were analyzed via LC injection into the mass spectrometer at a flow rate of 500  $\mu$ L/min (mobile phase A, H<sub>2</sub>O with 0.1% formic acid and mobile phase B, acetonitrile with 0.1% formic acid with a starting gradient at 95% A, 5% B). The mass spectrometer was operated in positive and negative ion mode. The LC column was a Thermo Hypersil Gold (50 mm  $\times$  2.1 mm, 1.9 um particle size) C4 column. The spectra were collected using the scanning range (100–1000) m/z. The assay included 10  $\mu$ M DHP, 500  $\mu$ M substrate, and 500  $\mu$ M H<sub>2</sub>O<sub>2</sub> in 5 mM KPi buffer pH 7 with a final volume of 250  $\mu$ L of reaction sample. The reaction was allowed to react for 15 min and quenched with catalase to stop the product formation. Data analysis was performed using Thermo Xcalibur software.

### 2.5. Protein crystallization and X-ray diffraction studies

Non-His tagged DHPA was overexpressed in Rosetta<sup>TM</sup>(DE3) pLysS competent cells (NOVAGEN) purchased from EMD Millipore Corporation (California, USA) and purified following established protocols [19,40-42] with some minor modifications. The protein was oxidized to the ferric state, before each experiment by adding excess amount of potassium ferricyanide and passing through the PD-10 (sephadex G-25) desalting column, to remove excess oxidizing agent. Crystals were grown using the hanging-drop vapor diffusion method with crystallization solutions at ratios of 1:1 and 2:1 of protein: reservoir solution in a volume of 5 mL. Crystals were formed in (30-32) % PEG 4000, 0.2 M ammonium sulfate, 0.02 M sodium cacodylate (pH 6.5) by mixing with 6 mg/mL protein dissolved in 20 mM sodium cacodylate (pH 6.5). Crystals grew after 3 days and were subsequently soaked overnight at 4 °C in precipitant solution supplemented with substrate at 40 mM and 80 mM of concentration containing 5% DMSO. After soaking, the crystals were cryoprotected with 25% glycerol added to the soaking solution and flash cooled and stored in liquid nitrogen until data collection. The

X-ray diffraction data were collected remotely at 100 K on the SER-CAT BM22 beamline using wavelength of 1.00 A° and a shutterless Rayonix MX300HS detector at Advanced Photon Source, Argone National Laboratories. The collected data were indexed, scaled, and integrated using the HKL2000 program suite [43]. The new crystals had the same space group (P212121) as the ferric metaquo structure form (PDB accession code: 2QFK) [44]. The structures were solved by molecular replacement using 20FK coordinates as a starting model with the Phaser molecular replacement program [45] and refinement is performed using REFMAC5 [46] in the CCP4 suite [47] and manual model building, and visualization is performed in COOT model building software [48]. Water molecules were placed into the refined structure in COOT molecular graphics software. The final models were validated using validation module in COOT and by using Molprobity [49] software. Data collection, processing and refinement statistics are summarized in Table S4, and structural figures are prepared with PyMol Molecular Graphics System, (version 1.2r3pre, Schrodinger, LLC).

#### 3. Results

# 3.1. Kinetic measurements of saturation curves based on the short time approximation

UV–visible spectrophotometric kinetic data were obtained for both substrates DCP and TCP in DHPA, DHPB, and HRP. The solvents used were aqueous phosphate buffer (referred as "in pH 7" in Fig. 3) or the same buffer containing 5% MeOH (referred as "in MeOH" in Fig. 3) to improve substrate solubility, since TCP and DCP are both sparingly soluble in water. The initial reaction rates,  $V_0$  were obtained by linear

regression of the initial 13 s of the kinetic measurement. Time-dependent single-wavelength kinetic data were obtained at 255 nm and 273 nm for products 2-ClQ and 2,6-DCQ of reactions with DCP and TCP, respectively. These rates were then plotted against substrate concentration in Fig. 3. Using these rates, the  $k_{cat}/K_m$  for each species (DCP, TCP and enzyme DHPA, DHPB, HRP) were evaluated and compared in Table 1.

DCP oxidation was compared to TCP oxidation at pH 7 to facilitate comparison with a large body of prior research [23,25,50-53]. The substrate pKa values of 6.1 and 7.9 are also factors that may affect the relative solubility of TCP and DCP, respectively [54,55]. Substrates like TCP bind near the  $\delta$ -edge of the heme in our reference enzyme, HRP [28]. However, both DCP and TCP bind in the distal pocket of DHPA and B to an extent depending on the dissociation constant, K<sub>d</sub>. Significant self-inhibition of peroxidase activity is observed for TCP in DHPA above 1.4 mM [53]. Self-inhibition is even more important in DHPB consistent with its lower  $K_d$  value of 210  $\mu M$  [10,56]. We can surmise that selfinhibition should be even more important for DCP, which has a very low  $K_d$  value of 29  $\mu$ M in DHPB [10]. The relative  $K_d$  has been measured using a competitive binding assay for fluoride in DHPA, providing a relative K<sub>d</sub> 5 times greater for TCP than DCP in DHPA [57]. The above values for DHPB give a ratio TCP:DCP of 7 for comparison [10,56]. Using  $K_d$  data for the mono-halophenols in DHPA [53] we estimate that  $K_d \sim$ 750  $\mu M$  for TCP and therefore  $K_d \sim 150~\mu M$  for DCP in DHPA. The 4–5 times higher binding affinity of substrates for DHPB relative to DHPA may be associated with the greater rates of reaction since substrate must be present when H<sub>2</sub>O<sub>2</sub> binds to initiate the reaction cycle. However, the concentration range of activity may be limited by self-inhibition by the substrates. While most previous assays of TCP have been conducting in

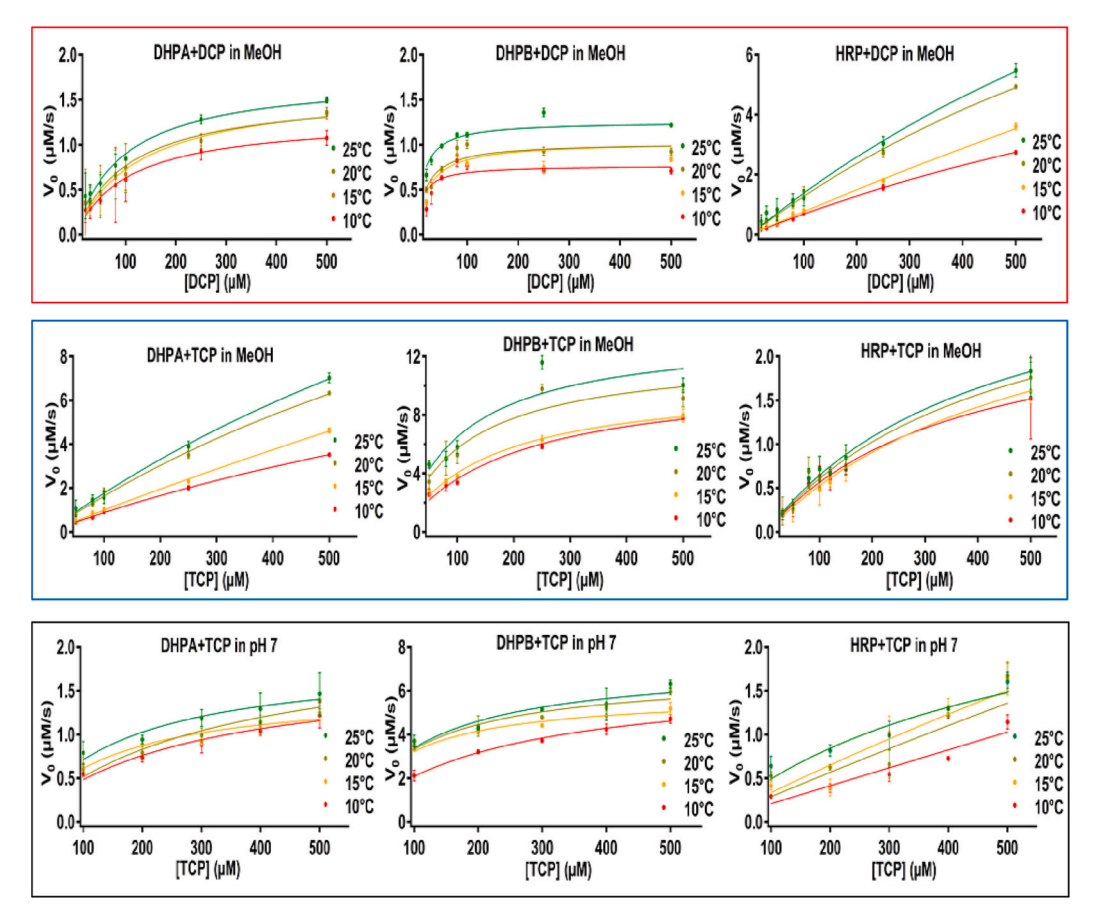


Fig. 3. Kinetic data for time-dependent UV–visible spectroscopic experiments for DHPA, DHPB and HRP with both substrates, TCP and DCP at 100 mM KPi pH 7 with and without 5% methanol and different temperatures (10 °C, 15 °C, 20 °C, 25 °C). Reaction condition: [DHPA] & [DHPB] = 2.4  $\mu$ M, [HRP] = 60 nM, [DCP] = (50–500)  $\mu$ M, [TCP] = (100–500)  $\mu$ M, [H2O<sub>2</sub>] = 1200  $\mu$ M.

 $\begin{tabular}{ll} \textbf{Table 1}\\ \textbf{Michaelis-Menten parameters for bench top mixing kinetic assay of DCP and TCP.} \end{tabular}$ 

Temperature	$k_{cat}$	$K_{m}$	k <sub>cat</sub> /K <sub>m</sub>	$k_1 (mM^{-1}$	$k_2 (mM^{-1})$
(°C)	$(s^{-1})$	(μM)	$(mM^{-1} s^{-1})$	s <sup>-1</sup> )	s <sup>-1</sup> )
DHPA+DCP in 5	5% MeOH				
10	0.545	108 $\pm$	$5.04 \pm 0.6$	0.227 $\pm$	27.7 $\pm$
	$\pm~0.0$	12.3		0.0	3.4
15	0.682	127 $\pm$	$5.39 \pm 1.0$	0.284 $\pm$	29.7 $\pm$
	$\pm~0.1$	21.1		0.0	5.4
20	0.660	108 $\pm$	$6.14 \pm 1.1$	0.275 $\pm$	33.8 $\pm$
	$\pm 0.1$	18.4		0.0	6.2
25	0.733	95.8 $\pm$	$7.65\pm1.2$	0.305 $\pm$	42.1 $\pm$
	$\pm~0.0$	13.9		0.0	6.6
DHPB+DCP in 5	5% MeOH				
10	0.319	$11.6~\pm$	$27.4 \pm 7.1$	0.133 $\pm$	151 $\pm$
	$\pm~0.0$	3.0		0.0	18.3
15	0.429	24.1 $\pm$	$17.8 \pm 1.4$	$0.179~\pm$	98.0 $\pm$
	$\pm~0.0$	1.9		0.0	7.9
20	0.427	19.6 $\pm$	$21.8 \pm 3.1$	0.178 $\pm$	$120\ \pm$
	$\pm 0.0$	2.7		0.0	16.8
25	0.524	13.5 $\pm$	$38.9 \pm 3.2$	0.218 $\pm$	214 $\pm$
	$\pm~0.0$	1.1		0.0	17.6
HRP + DCP in 5	5% MeOH				
10	NA	NA	$121 \pm 4.1$	NA	$669 \pm 9.8$
15	NA	NA	$133 \pm 9.3$	NA	730 ±
10			100 ± 510		12.7
20	NA	NA	$229 \pm 7.9$	NA	1260 ±
20			22, 1,,,		10.2
25	NA	NA	$145 \pm 9.9$	NA	1340 ±
					21.7
DHPA+TCP in 5					
10	5.94 ±	1530 ±	$3.89 \pm 1.0$	2.47 ±	$21.4 \pm$
	1.1	321		0.4	5.7
15	$20.2 \pm$	4780 ±	$4.23\pm3.0$	8.41 ±	23.3 ±
	3.0	336		1.2	16.7
20	9.21 ±	1260 ±	$7.32\pm1.8$	3.84 ±	40.2 ±
0.5	1.5	235	7.05   0.0	0.6	10.0
25	$11.2 \pm \\3.5$	$1420 \pm 565$	$7.85 \pm 3.9$	$4.65 \pm 1.5$	$43.2 \pm 21.8$
DHPB+TCP in 5	5% MeOH				
10	4.48 $\pm$	$197~\pm$	$22.8\pm2.7$	$1.87~\pm$	$125~\pm$
	0.2	21.4		0.1	14.9
15	4.32 $\pm$	157 $\pm$	$27.5 \pm 4.8$	1.80 $\pm$	151 $\pm$
	0.4	24.4		0.1	26.4
20	5.07 $\pm$	$113~\pm$	$44.8\pm10.5$	2.11 $\pm$	246 $\pm$
	0.4	25.0		0.2	58.0
25	5.67 $\pm$	110 $\pm$	$51.8 \pm 6.5$	2.36 $\pm$	285 $\pm$
	0.3	12.6		0.2	36.0
HRP + TCP in 5	5% MeOH				
10	NA	NA	$120\pm4.1$	NA	$658 \pm 6.0$
15	NA NA	NA NA	$120 \pm 4.1$ $104 \pm 4.2$	NA NA	$573 \pm 6.3$
20	NA	NA	$125 \pm 5.8$	NA	$689 \pm 9.7$
25	NA	NA	$134 \pm 7.1$	NA	732 ±
20	1471	1421	101 ± 7.1	1411	11.6
DHPA+TCP in p					
10	0.858	$372 \pm$	$2.31\pm0.3$	$0.358 \pm$	12.7 $\pm$
	± 0.1	39.2		0.0	1.6
15	0.742	269 ±	$2.76\pm0.5$	0.309 ±	15.2 $\pm$
	$\pm 0.1$	45.2		0.0	2.9
20	0.891	316 ±	$2.82\pm0.5$	0.371 ±	15.5 ±
0.5	$\pm 0.1$	45.2	488	0.0	2.7
25	0.774	162 ±	$4.77\pm3.0$	0.323 ±	26.2 ±
	$\pm 0.1$	94.5		0.1	16.4

DHPB+TCP in pH 7

Table 1 (continued)

Temperature (°C)	$k_{\text{cat}} \ (s^{-1})$	K <sub>m</sub> (μM)	$\begin{array}{c} k_{cat}/K_{m} \\ (mM^{-1} s^{-1}) \end{array}$	$k_1 \text{ (mM}^{-1} \text{ s}^{-1}\text{)}$	$k_2  (mM^{-1} \ s^{-1})$
10	$2.77~\pm$	220 ±	$12.6\pm2.3$	$1.15 \pm$	69.3 ±
	0.2	36.4		0.1	12.4
15	2.44 $\pm$	81.7 $\pm$	$29.9 \pm 1.6$	$1.02\ \pm$	$164 \pm 8.5$
	0.1	3.9		0.1	
20	2.83 $\pm$	105 $\pm$	$27.0 \pm 4.5$	1.18 $\pm$	148 $\pm$
	0.1	17.2		0.1	24.9
25	3.03 $\pm$	$115~\pm$	$26.3 \pm 7.0$	$1.26~\pm$	144 $\pm$
	0.2	29.3		0.1	38.2
HRP + TCP in p	ЭН 7				
10	NA	NA	$34.5 \pm 0.0$	NA	$189 \pm 0.3$
15	NA	NA	$57.3 \pm 5.4$	NA	$315\pm2.1$
20	NA	NA	$48.5 \pm 2.2$	NA	$267\pm1.4$
25	NA	NA	$97.9 \pm 2.1$	NA	$538 \pm 6.4$

the substrate concentration range from 100 to 1500  $\mu$ M, because of the relatively low K<sub>d</sub> found for DCP the range in this study was from 30  $\mu$ M to 500  $\mu$ M.

The saturation curves and linear dependence of HRP shown in Fig. 3 provide a common basis for measurement of the rate constants  $k_1,\,k_2$  and  $k_3$  for the two isoforms of DHP as explained in Eqns. S1-S15 of the Supporting Information. The values of  $k_{cat}$  and  $K_m$  were not uniquely determined for HRP because all data are in the linear range well below saturation, but the ratio  $k_{cat}/K_m$  is still defined.

# 3.2. Temperature dependent UV-visible studies of DCP and TCP oxidation

We can see in the kinetic data in Fig. 3 that there is temperature dependence for the initial rate of the DCP oxidation reaction. All three enzymes show an increasing trend in rate from 10 °C to 20 °C. The maximum rate for all species is observed at 25 °C but is significantly reduced at 30 °C with HRP showing the greatest rate decrease. One likely explanation is that the enzymes may partially denature in 5% MeOH at 30 °C and accordingly, the data at 30 °C were not included in this analysis. The sensitivity of HRP to denaturation may be heightened in solutions of TCP.

Table 2 shows the results obtained from an Arrhenius plot of each temperature-dependent data set. For TCP oxidation reaction, DHPA and DHPB have similar activation energies, E<sub>a</sub> in aqueous buffer and higher Ea in 5% MeOH/buffer. The activation energy of TCP oxidation by HRP is 6 times lower in 5% MeOH buffer solution than in buffer solution, which is likely a result of incipient HRP denaturation under these conditions, particularly at the higher temperatures. The activation energies for DCP oxidation by DHPA and DHPB are 19.3  $\pm$  2.5 and 24.3  $\pm$  3.2 kJ/ mol, respectively. The corresponding activation energies for TCP in 5% MeOH/buffer are 37.2  $\pm$  6.5 and 41.4  $\pm$  4.5 kJ/mol, which may be higher due to the greater solvent exposure of the TCP, which binds externally under these conditions. The activation energy of TCP oxidation by DHPA is 30.7  $\pm$  7.2 kJ/mol, which is smaller than the value of 44 kJ/mol measured previously [18]. However, the 95% confidence limits are larger in aqueous buffer, probably because of the difficulty of dissolving TCP in a consistent manner due to its poor solubility.

**Table 2**Activation energy for DHP catalyzed oxidation of DCP and TCP.

Activation Energy E <sub>a</sub> , (kJ/mol)			
	TCP Oxidation		DCP Oxidation
Enzymes	5% MeOH	pH 7	5% MeOH
DHPA	$37.2 \pm 6.5$	$30.7 \pm 7.2$	$19.3\pm2.5$
DHPB	$41.4 \pm 4.5$	$29.9 \pm 15.3$	$24.3\pm3.2$
HRP	$7.0\pm4.4$	$\textbf{41.5} \pm \textbf{11.2}$	$37.2 \pm 6.5$

Note: The error estimation represents the  $\pm 95\%$  confidence interval.

Nonetheless, the activation energy for oxidation of TCP and DCP is larger for HRP than DHPA or B, except the TCP substrate in 5%MeOH/buffer mentioned above. According to the hypothesis the larger values are consistent with external binding in HRP.

The reorganization energies,  $\lambda$ , in Table 3, were calculated based on the measured activation energies,  $E_a$  in Table 2 and driving forces,  $\epsilon$ , in Eq. S18. In terms of the oxidation reaction of DHP and DCP, the thermodynamic driving force for the reaction of compound I with reducing substrate is the difference between the mid-point potentials of compound I/compound II and DCP radical/DCP couples. Two different experimental approaches provide  $\epsilon$ , 1.) calomel electrode electrochemistry and 2.) pulse radiolysis relative to the standard hydrogen electrode.

The measured mid-point potential for compound I/compound II was 0.879 V at pH 7 in standard hydrogen electrode in pulse radiolysis in HRP [35] and oxidation potential for DCP and TCP is 0.55 V and 0.76 V respectively using the standard calomel electrode [38]. In the first approach, the data obtained from the calomel electrode for chlorophenols were converted into the standard hydrogen electrode by the addition of 0.241 V to the calomel electrode potential of each respective chlorophenol. These corrected potentials were used to calculate the driving force. In the second approach, the mid-point potentials of compound I/compound II and chlorophenol were taken into account from pulse radiolysis. Pulse radiolysis data were available only for p-Cl phenol. The reduction potential was 0.94 V using pulse radiolysis. Hence the value for p-Cl phenol is used for both substrates, which is clearly only an estimate. An interpretation of the magnitude of the reorganization energy must account for the fact that the process measured is a protoncoupled electron transfer. The goal of this analysis is to find the relative magnitude of the reorganization energy for various substrates and enzymes as shown in Table 3.

#### 3.3. Effects of polymerization on kinetic observations

DCP oxidation by HRP results in significant polymerization, which complicates the comparison. Indeed, there is a small yield of multimers and polymers under all conditions, but this is not large for DHPA and B because the substrate DCP binds internally and TCP is protected in both ortho and para positions. While mass spectrometry shows the existence of multimers formed by radical reactions [10] it is difficult to obtain an estimate of the polymerization yield because of precipitation. We investigated the polymerization yield by applying singular value decomposition (SVD) to the spectrophotometric time-resolved data. Figs. S4-S9 in the Supporting Information show the spectral and time components of the two important SVD basis spectra. Table S1 provides the single exponential fits to the components. This is consistent with parallel process that we have interpreted as an increase in background absorbance due to scattering for the first component and the productreactant difference spectrum for second component. The scattering background in first component is thought to arise from polymerization. The second component arises from the enzymatic conversion of phenol to quinone. There is a substantial difference between DHP and HRP that is evident in the SVD study. Table S2 shows weighted amplitudes for

**Table 3** Reorganization energies for DHP and HRP.

Reaction Condition	Reorganization Energy, λ (eV)		
	Corrected Calomel Electrode	Pulse radiolysis	
DHPA+DCP (5% MeOH)	0.97	0.92	
DHPB+DCP (5% MeOH)	1.18	1.13	
HRP + DCP (5% MeOH)	1.72	1.67	
DHPA+TCP (5% MeOH)	1.78	1.67	
DHPB+TCP (5% MeOH)	1.96	1.84	
HRP + TCP (5% MeOH)	0.51	0.40	
DHPA+TCP (pH 7)	1.51	1.40	
DHPB+TCP (pH 7)	1.48	1.38	
HRP + TCP (pH 7)	1.96	1.85	

each SVD component compared for three enzymes. HRP has a significantly more rapid and significant first component when DCP is the substrate associated with significant polymerization. DHPA and B timeresolved spectra for DCP oxidation have two components with time courses that are nearly identical. This result suggests a single process dominated by oxidation of the phenol to a quinone. The amplitude of the first component is significantly smaller when TCP is the substrate. The yields of polymerization of DCP and TCP are approximately 60% and 17%, respectively, in HRP by this analysis. Based on the SVD analysis we conclude that use of the short-time approximation presented in Table 1 is valid for both isoforms of DHP. However, the HRP kinetic data for DCP oxidation show significant polymerization. These data are also the most problematic for the Arrhenius analysis because the protein appears to denature in 5% MeOH/buffer solutions. The binding and reactivity of TCP in DHPA has been studied previously by these methods and the data are consistent with binding of TCP in the phenolate form, precisely as observed in HRP. The spectra of the phenolate forms with absorption bands at 314 nm and 249 nm can be seen in HRP and DHPA in Figs. S7 and S8. It is known that TCP binds internally in the distal pocket of DHPA at higher concentration, but at 500 mM it is expected to be in the phenolate form as observed in Fig. S8. The surprising finding in the SVD analysis is that the initial spectrum of substrate TCP appears to be primarily in the phenol form in the DHPB spectrum in Fig. S9. It is not possible to prove that the phenolate form binds externally, but it seems unlikely that a charged molecule would bind in the hydrophobic distal pocket. On the other hand, the phenol form would be expected for internal binding. This suggests that the mode of binding of TCP substrate could be quite different in DHPA and DHPB.

# 3.4. HPLC reactivity studies of effects of secondary oxidation on kinetic observations

It has been reported previously that 2,6-DCQ, the oxidation product of TCP, remains stable below 10 °C and a secondary hydroxylation reaction takes place above this temperature [18]. The secondary oxidation process is not enzymatic and occurs in control experiments with 2,6-DCQ as a substrate in the presence of  $\rm H_2O_2$ . The  $\rm H_2O_2$  dependent reactions of ferric DHPA and 2,4-DCP and 2,6-DCP were monitored by HPLC at pH 5, 6, 7 and 8 and the percentage of corresponding substrate conversion (i.e., substrate loss) is reported in Table 4. The reaction was started with addition of 500  $\mu M$  H<sub>2</sub>O<sub>2</sub> to a 5% MeOH/buffer solution of 10  $\mu M$  DHPA, 500  $\mu M$  DCP mixer in 4 different pHs and quenched with catalase after 5 min. Non-enzymatic (no DHP) and non-oxidative (no H<sub>2</sub>O<sub>2</sub>) control reactions were also run. The chromatograms were observed at 255 nm.

The data in Table 4 reveal that the percent conversion is higher at pH 7 than pH 5 for both substrates. Because 2,4-DCP had the highest conversion rate at pH 7, this substrate and pH were selected for studies of the secondary oxidation reaction by HPLC using 255 nm as the detection wavelength [58]. Since this is the only experiment in which 2,6-DCP was studied we refer to DCP as the acronym for 2,4-DCP elsewhere in this manuscript. The chromatogram for the DHPA catalyzed reaction of DCP in the presence of  $\rm H_2O_2$  is shown in Fig. 4. The chromatogram also shows the formation of 2-ClQ as a product which elutes with 5.8 min retention time confirmed by the retention time of a 2-ClQ standard under the same

**Table 4** DHP catalyzed studies for oxidation of substrate. The reaction was initiated by the addition of 500  $\mu$ M of  $H_2O_2$  to a solution of 10  $\mu$ M ferric DHPA, 500  $\mu$ M subsrate in 5% MeOH/100 mM KP<sub>1</sub> buffer pH 7. The reaction was quenched with catalase after 5 min.

Substrate	Conversion (%)			
DHPA WT Ferric +	pH 5	pH 6	pH 7	pH 8
2,4-DCP	14.8	26.5	53.0	29.6
2,6-DCP	14.3	31.4	41.3	26.5

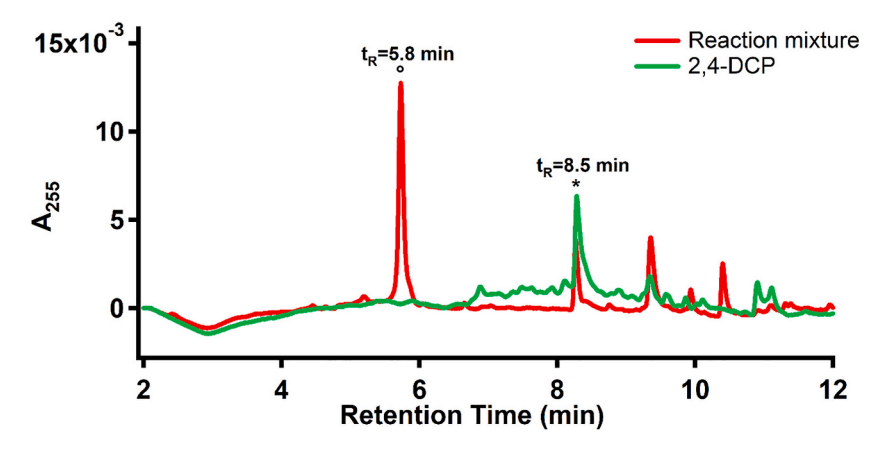


Fig. 4. HPLC chromatograms for reaction of DHPA with DCP in the presence of  $H_2O_2$ . Reaction condition: [ferric DHPA] =  $10 \mu M$ , [2,4-DCP] =  $500 \mu M$  and  $[H_2O_2]$  =  $500 \mu M$  at 100 m M KPi buffer pH 7 with 5% MeOH quenched with catalase after 5 min. Asterisk indicates 2,4-DCP peak. Percent conversion~53%.

experimental conditions (data not shown). The substrate peak is observed at 8.5 min retention time. As observed in previous studies, neither substrate turnover nor product formation were observed in control experiments that lacked either  $\rm H_2O_2$  or DHP enzyme.

#### 3.5. Product identification By LC-MS

The 2-ClQ and secondary product were further analyzed by LC-MS. Relevant peaks ++were detected by negative ion mode for both enzymes; DHPA and DHPB and three main peaks were observed in different reaction samples. The species, in order of retention time, were DCP, 2-ClQ and hydroxylated quinone, 2-ClQOH. 2-ClQOH is the product of a secondary hydroxylation reaction that takes place after the oxidation reaction of DCP and the evidence and data for this reaction will be presented in a separate manuscript. The retention times in HPLC and LC-MS depend on different column composition (C18 for HPLC and C4 for LC-MS), but the order of the retention time of the species is the same. The peaks with retention times of 1.8 min for 2-ClQOH, 5.8 min for 2-ClQ and 8.5 min for 2,4-DCP in HPLC correspond to 0.5 min, 1.6 min, and 2.3 min in LC-MS, respectively. The data in last two rows of Table S3 confirms that 2,4-DCP in the control with H2O2 in absence of the enzyme does not form 2-ClQ or 2-ClQOH. This result compliments the HPLC data obtained previously. The evidence for the secondary hydroxylation reaction will be presented in a future manuscript (Fig. 5).

### 3.6. X-ray crystal structure of bound DCP in DHPA

The crystal structure for non-His tagged WT DHPA in a complex with substrate 2,4-dichlorophenol (DCP) was determined at a resolution of 1.48  $\mathring{A}$ . DHPA. Two protomers in the unit cell were observed per asymmetric unit as in every prior DHP crystal structure. The protomers are labeled A and B by convention. This presents the potential for ambiguity since both DHPA and DHPB possess these two protomers. The unit cell was  $P2_12_12_1$  as observed previously [59]. The structure was deposited to the RSCB protein database with the PDB accession number of 8EJN. The X-ray data collection and refinement statistics are listed in

Fig. 5. Chemical structure of the major peaks in negative ion mode LC-MS.

Table S4 and selected distances are listed in Table 5.

The substrate 2,4-DCP was found to bind internally in chain A of the asymmetric subunit shown in Fig. 6. It was found to bind in two conformers with equal partial occupancy of 30%. In a third conformer that lacks 2,4-DCP there is a water molecule bound to the heme molecule with the same partial occupancy of 30%. When the DCP is bound in the distal pocket, H55 is in the open conformation, but when  $\rm H_2O$  is bound to Fe H55, it is observed in the closed (internal) conformation.

The  $F_o$ - $F_c$  map shows where the experimentally observed density disagrees with the atomic model. Negative density is shown in red (atoms in the model that lack electron density) and positive density in green (excess electron density lacking an atomic model). The electron density map in the blue color in Fig. 6 is the  $2F_o$ - $F_c$  map contoured at  $1\sigma$  level that shows how well the electron density fits the atomic model and green color density indicates  $F_o$ - $F_c$  map contoured at  $3\sigma$  level.

Based on the electron density, two distinct conformations of DCP binding shown in Fig. 6 were observed with  $\sim\!0.3$  occupancy each. When substrate fitting was performed in the DCP<sub>A</sub> conformation, with a partial occupancy of 30%, there was excess density that appeared to correspond to a second conformation, which also fits in the density with a partial occupancy of 30%. Hence, another binding conformation as DCP<sub>B</sub> was proposed. So, in total 3 conformations of nearly equal occupancy were observed; (1) Closed conformation of H55 H-bonded to water, (2) DCP<sub>A</sub> and open conformation of H55 and (3) DCP<sub>B</sub> and open conformation of H55. In Fig. 6, each panel shows 2 conformations of the substrate separately.

Fig. 7 shows the crystal structure for DHPA with the two conformations of 2,4-DCP binding internally with the binding site being located above the heme plane toward the beta edge of the heme pocket.

Fig. 8 shows DCP along with neighboring amino acids. DCP is oriented to have favorable interaction by  $\pi$ -stacking with F21. The Cl atoms are positioned internally while the OH groups are directed toward heme edge, at a hydrogen bonding distance from propionate group D. When

**Table 5**Selected distances (Ångströms) for DHPA-DCP complexes (protomer A).

PDB entry	8EJN
Substrate occupancy	A, 30% / B, 30%
Distal H <sub>2</sub> O occupancy	40%
Fe distal H <sub>2</sub> O	2.28
F21 $C^{\epsilon \dots C^3}$ (DCP)*	$3.06_{\rm B}/{\rm C}^5-2.98_{\rm B}$
F21 C <sup>ζ</sup> C <sub>2</sub> (DCP)*	$4.01_{\rm B}/{\rm C}^6-3.75_{\rm B}$
Distal H <sub>2</sub> O······H55 N <sup>ε</sup>	3.68
Fe·····H89 N <sup>ε</sup>	2.10

 $<sup>^{*}</sup>$  The 2,4-DCP conformations are denoted with subscript DCP<sub>A</sub> and DCP<sub>B</sub> as in Fig. 6.

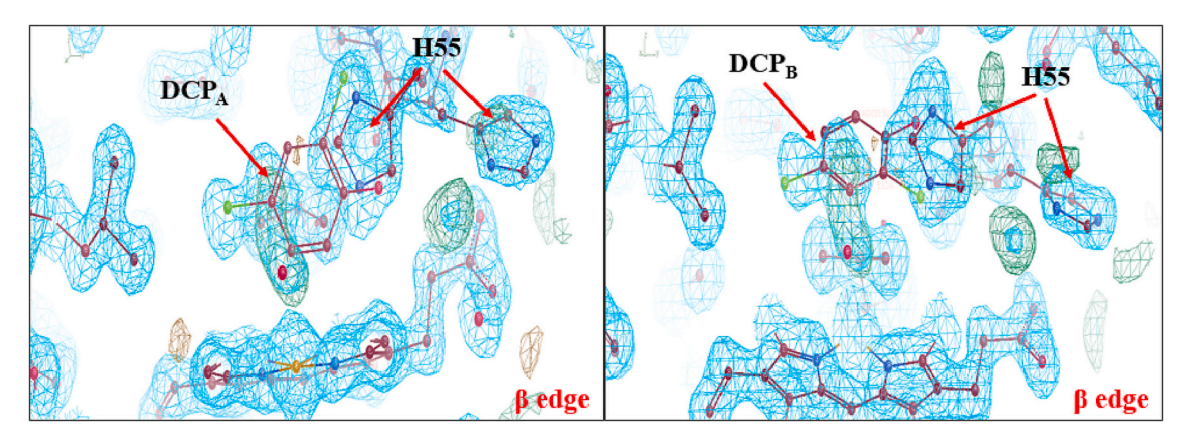


Fig. 6. Two different conformations of DCP binding (DCP<sub>A</sub> and DCP<sub>B</sub>) with DHPA (PDB ID 8EJN). Each panel shows 2 conformations. The internal or closed conformation of H55 has an occupancy of 0.3. The occupancies of the DHP<sub>A</sub> and DCP<sub>B</sub> are both  $\sim$ 0.3.

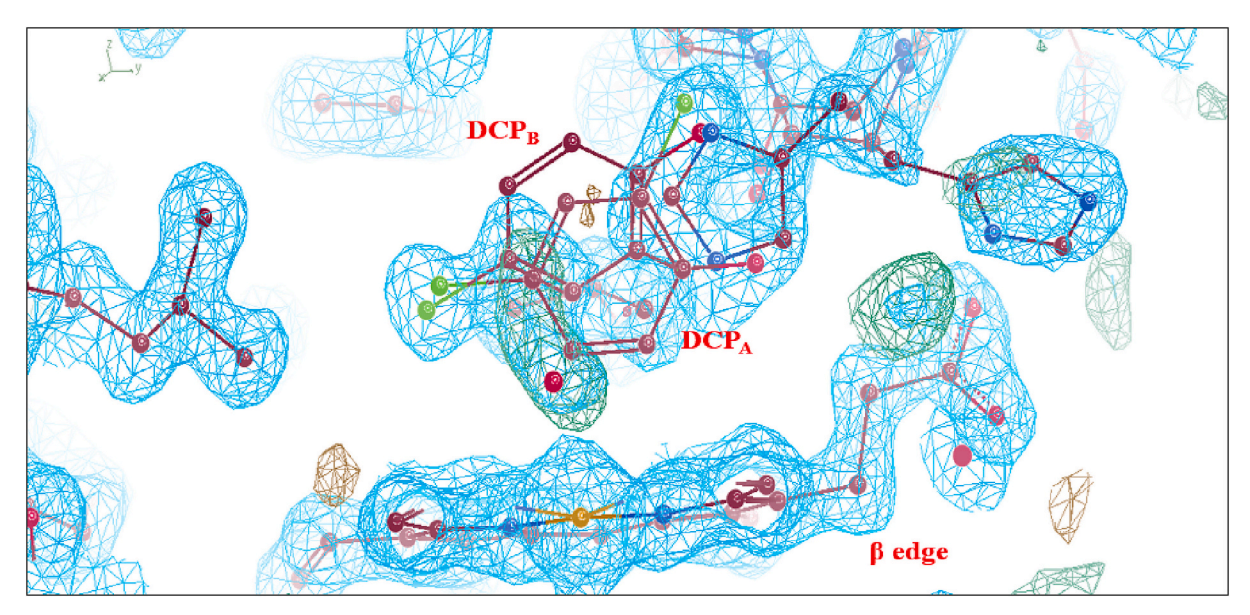


Fig. 7. Crystal structure of DHPA and DCP with all possible binding conformations (PDB ID 8EJN).

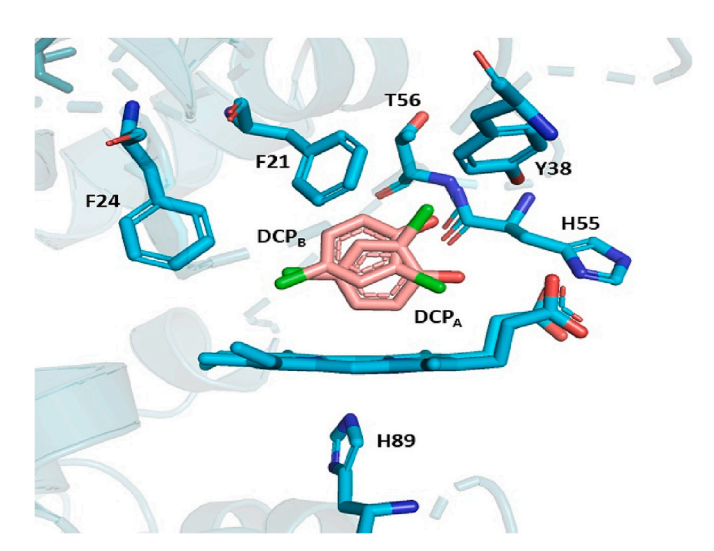


Fig. 8. Crystal structure of DHPA and DCP showing the two binding conformations of the substrate as well as the neighboring amino acids (PDB ID 8EJN).

DCP is bound inside, H55 is in open conformation and Fe-ligated water molecule is not present. The p-Cl atom in both conformations of DCP substrate orients to occupy the Xe1 binding site [60].

#### 4. Discussion

We have used the standard enzyme kinetic saturation model, based on the Michaelis-Menten model in Reaction Scheme 1 in the Supporting Information, to obtain parameters  $k_{\text{cat}}$  and  $K_{\text{m}}$  shown in Fig. S2. This model is useful because it is mathematically related to the peroxidase reaction scheme, which permits us to obtain quantitative values for k<sub>1</sub>, k<sub>2</sub>, and k<sub>3</sub> rate constants of the peroxidase reaction scheme as shown in both Fig. 1 and Reaction Scheme 2. The rate constant  $k_1 = k_{cat}/[H_2O_2]$ . Rate constants  $k_2$  and  $k_3$  are proportional to  $k_{\text{cat}}/\ K_m$  as shown in Eqns. S12-S15. The comparison of two distinct substrates and different peroxidases permits one to dissect the significance of the rate constants in the peroxidase reaction scheme. The peroxidase scheme has three steps, 1.) activation by co-substrate  $H_2O_2$  binding to Fe, with rate constant  $k_1$ , 2.) a first electron transfer from substrate to the heme oxo-radicalcation, with rate constant k2, and 3.) a second electron transfer from substrate to the heme-oxo intermediate to return to the resting state, with rate constant k<sub>3</sub>, also shown in Fig. 1. There have been relatively few studies of the electron transfer rate constants in peroxidase enzymes

in terms of Marcus theory [36]. Perhaps, this is because the structural evidence has placed substrates near the heme edge, but without a clearly identified geometry. The interpretation is more involved because the processes are actually proton-coupled electron transfer reactions. The relative magnitude the reorganization energy in DHPA and DHPB relative to HRP provides additional evidence that certain substrates bind internally in the distal pocket.

The activation step involving binding of  $\rm H_2O_2$  and rearrangement to form a heme-oxo intermediate is similar in all peroxidases, although the magnitude of the rate constant  $\rm k_1$  varies considerably. The initially formed intermediate, Cmpd I, is an iron-oxo heme radical cation. Some peroxidases undergo a rapid electron transfer between an amino acid in the protein and the heme radical cation to form an amino acid radical cation, usually to form tryptophanyl or tyrosyl radical. DHPA and B are both examples of this type of behavior. There is evidence for several tyrosyl radicals in a species that is analogous to compound ES of cytochrome c peroxidase [25,61]. The differences in the activation step may be related to differences in reactivity of the various forms. Examination of Table 1 provides an estimate of the relative activation rate constants.

These results are consistent with prior research. First, we observe that the magnitude of  $k_{cat}/K_m$  for DHPA at pH 7 and 25 °C is reported in previous studies as  $5.05 \pm 0.08 \text{ mM}^{-1} \text{ s}^{-1}$  [53],  $6.63 \text{ mM}^{-1} \text{ s}^{-1}$  [18], 4.0mM<sup>-1</sup> s<sup>-1</sup> [62] which are in reasonable agreement with our measurement of 4.77  $\pm$  2.98 mM<sup>-1</sup> s<sup>-1</sup>. Second, the reaction rate constant, k<sub>2</sub> is higher for DHPB than DHPA for both DCP and TCP oxidation reactions. While the greater catalytic efficiency, k<sub>cat</sub>/K<sub>m</sub>, for DHPB was observed previously, the correspondingly faster electron transfer is confirmed in the present research. The reaction rate is 3.5 times greater in DHPB than DHPA for DCP, 6 times greater for TCP in DHPB with 5% MeOH/buffer, and nearly 10 times greater for TCP in DHPB in buffer solution. The catalytic efficiency has been reported to be 2.6-fold higher in DHPB than DHPA at pH 7 by D'Antonio and coworkers and 8 times higher by Maduresh and coworkers [62,63]. The differences in rate of electron transfer in DHPA and B may depend on the differing number of tyrosines in the two proteins [25,62,64]. Several oxidized tyrosines can participate in the formation of a compound ES [25]. The crucial amino acid, Y34, is not present in DHPB and the charge hopping pathway is different in DHPA and DHPB. The distances affect the rate of the  $k_2$  electron transfer process. Tyrosines are known to affect through-bond and through-space coupling in protein electron transfer and these effects may affect k3. Since DCP binds internally, it may compete with formation of compound ES. The fact that amino acid 34 is a tyrosine (Y34) in DHPA and asparagine (N34) in DHPB may affect this competition and play a role in the relative rates of electron transfer.

The electron transfer rate constants k2 and k3 in Table 1 were obtained by analysis of k<sub>cat</sub>/K<sub>m</sub>. In Following Folkes and co-workers we assumed that k2 is ten times larger than k3 [35]. This result is consistent with the similarity in the electron transfer processes in HRP. In a general model the relative rate is expressed as the parameter  $\alpha$ ,  $k_2 = \alpha k_3$ . To obtain a numerical value we have assumed that  $\alpha = 10$  to give Eq. 1, based on the finding by Folkes and co-workers for many phenolic substrates. The general derivation results in Eq. S15 in the Supporting Information. The electron transfer rate constants have been compared for DHPA, DHPB, and HRP. From the X-ray crystal structures and other data it is clear that internal binding should have a large effect on the rate of electron transfer and therefore the overall peroxidase mechanism. HRP provides an experimental control in the sense that external substrate binding is well-established. We have compared the electron transfer rate constants for DHPA and DHPB accounting for internal binding of DCP and possible internal and external binding of TCP. The role of solvent was compared to determine the effect when 5% MeOH was added to solubilize the substrates. Finally, we have used an activation energy obtained from the Arrhenius equation to estimate the reorganization energy for the various enzymes, which provides information on the solvation environment of reacting substrates.

The electron transfer rate constants, k2 and k3, are dependent on

solvent reorganization energy which differs for external and internal substrate binding. The reorganization energy of externally bound substrate should be lower in 5% MeOH/buffer than aqueous buffer due to a reduction in the dielectric constant of the solvent mixture. These effects may be non-linear because MeOH will tend to sequester a hydrophobic solute as well. Hence, the reorganization energy would be predicted to be lower in in a 5% MeOH solvent mixture. Assuming that the electron transfer is in the normal region of Marcus theory where  $\varepsilon < \lambda$ , lowering  $\lambda$ also lowers the activation energy. Table 3 shows that there is a significant difference in reorganization energy between DCP and TCP. For transfers involving DCP as a donor,  $\boldsymbol{\lambda}$  is 1.5 times smaller for DHPA and DHPB than for HRP which is consistent with the notion that DCP binds outside in HRP and inside in DHP. The protein dielectric function should be considerably lower than 5% MeOH/H2O even with preferential MeOH solvation of the hydrophobic substrate [25,65]. This also complements the observed internal substrate binding geometry in the crystal

If DCP binds to the surface of HRP, consistent with previous studies [66], and is surrounded by a hemisphere of water then it will have larger reorganization energy than DCP bound inside the distal pocket of DHPA and DHPB. This structural picture can explain why DHP A and B have smaller reorganization energies than HRP. The outer sphere reorganization energy has been estimated to be in the range of 0.5–1.25 eV in case of peroxidases [18,35,67]. In Table 3, some of the reorganization energies are larger than this range, perhaps because of systematic error in comparing energies obtained from an Arrhenius plot to electrochemical measurements of the thermodynamic driving force. Nonetheless, the trends in the reorganization energies provide a basis for inferring different modes of substrate binding. The exception is HRP in 5% MeOH/buffer solution. The very small activation energy in that case may result from the onset of protein denaturation under these conditions.

The distance dependence of the electron transfer rate is another important factor that may be affected by the binding site of the substrate. The distance dependence is described in the Supporting Information section S.3 and Eq. S17. The electron transfer rate constant decreases exponentially with distance because of reduced overlap of reactant and product wave functions given in the electronic factor. If the substrate binds inside the heme pocket, the reaction rate will also be increased relative to external binding due to the shorter distance. This can be a large effect since the difference in distance can be  $>\!3\,\text{Å}$ , which gives a reduction in at least a factor of 10 in the electron transfer rate constant.

The superimposed crystal structures of 4-nitrophenol (4-NP), tribromophenol (TBP), internally bound trichlorophenol (TCPent), dichlorophenol (DCP) and 4-bromophenol (4-BP) shown in Fig. 9 demonstrate the range of binding conformations from the  $\alpha$ - and  $\beta$ -, to the γ-site. 4-BP is a peroxidase inhibitor, binds directly above the heme-Fe and inhibits  $H_2O_2$  activation in the  $\beta$ -site [68]. Peroxygenase substrate 4-NP, whose binding site is positioned close to the heme center in a conformation slightly higher than the  $\beta$ -site allows direct O atom insertion from the ferryl intermediate. The binding site is slightly different for 4-BP than 4-NP but they bind close to each other. This slightly different binding results in a significant difference in catalytic activity. The DCP binding site in DHPA is closer to the heme than 4-BP and 4-NP and 4-BP and 4-NP is oriented higher above the heme. The p-Cl atom in both conformations of DCP are well positioned in the Xe1 binding cavity region which is consistent with other halogenated substrates such as 4-BP [68], TBP [53], 4-bromo-o-cresol [69], 4-bromo-oguaiacol [15]. DCP binds in an intermediate positions between TCP and TBP binding modes.

Malewschik et al. also reported two conformations of DCP binding internally with DHPB (7LZK for DCP $\beta$  and 7LZN for DCP $\alpha$ ) [10]. The superimposed crystal structures of DHPA and DHPB with DCP shows that DCP $\alpha$  conformation of DHPB (7LZN) are identical with DCP $_B$  conformation of DHPA shown in Fig. S10. Another crystal structure of

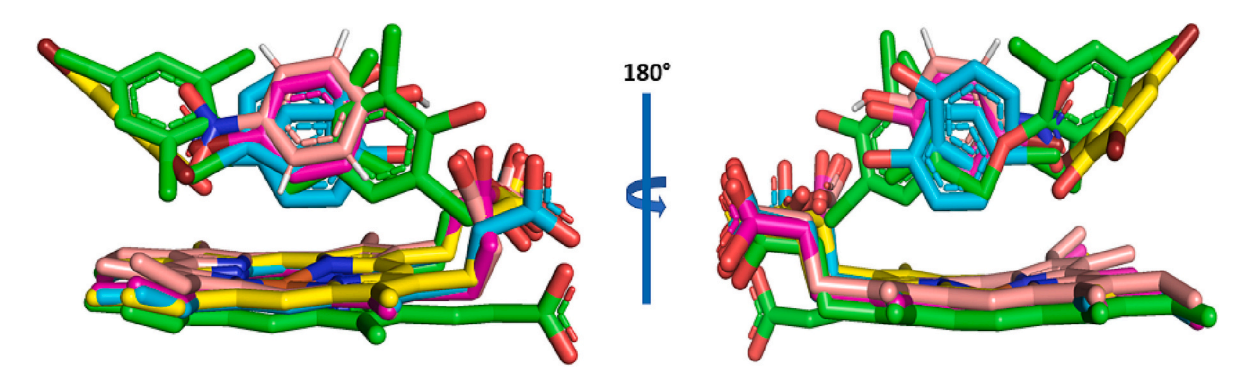


Fig. 9. Superposition of selected substrates of DHP. Binding site superposition is shown for TBP (yellow, PDB entry 4FH6) [53], TCPent and TCPext (green, PDB entry 4KN3) [51], 4-NP (light coral, PDB entry 5CHQ) [16], 4-BP (purple, PDB entry 3LB2) [68], and DCP (cyan, PDB entry 8EJN). (For interpretation of the references to color in this figure legend, the reader is referred to the web version of this article.)

DHPB complexed with DCP (PDB: 617F) was recently determined by Moreno-Chicano et al. by serial femtosecond x-ray crystallography (Fig. S12) [70]. They observed only one binding conformation for DCP which significantly differs from the observed positions for DCP<sub>A</sub> and DCP<sub>B</sub>. The variety of conformations observed are consistent with the great solvent accessibility of the distal pocket of DHP. The conformations may result in changes in function since the conformation required for peroxygenase chemistry requires a specific distance and orientation between the heme iron and C—H bond. The peroxidase mechanism can function both for externally and internally bound substrates as long as they do not conflict with the binding of co-substrate, H<sub>2</sub>O<sub>2</sub>.

#### 5. Conclusion

The temperature dependence of the initial rate of the DCP oxidation reaction provides an estimate of the activation energy and, by extension, the reorganization energy for each isoform of DHP in comparison with HRP. DHPA and B have similar reorganization energies and electron transfer driving forces for both TCP and DCP substrates. The catalytic efficiency,  $(k_{\text{cat}}/K_{\text{m}})$  is 3.5 times higher for DCP oxidation in DHPB than DHPA, which may be a function of the mode of binding of DCP in the distal pocket, which was observed to differ in significant ways by crystallographic structure determination. DCP shows self-inhibition even at modest concentration (<0.2 mM).

Based on this study, DCP binds tightly inside the heme pocket of DHPA in two conformations, which are different from DHPB, although both show high occupancy for internalized DCP substrates. The three chlorinated phenols, TCP, 4-CP and DCP bind in three different sites, mainly  $\alpha$ ,  $\beta$ - and  $\gamma$ -sites, respectively, but also an additional internal site in the case of DCP. Moreover, the binding heterogeneity of DCP in the DHPA and B isoforms may affect electron transfer rates and even mechanism. A fraction of the substrates undergoes peroxygenation in DHPB. Similar trends exist for the brominated analogs of each of these molecules. These have great relevance to the marine ecosystem but are correspondingly difficult to study because of the low solubility of brominated substrates. Chlorinated phenols provide versatile models of the multi-functional nature of DHPA and B.

### **Author statement**

Time-dependent spectroscopic kinetic experiments were conducted by Mst Sharmin Aktar. The X-ray crystals were grown and structure determined by Mst Sharmin Aktar with significant guidance by Vesna de Serrano. The kinetic analysis was conducted by Mst Sharmin Aktar with guidance by Stefan Franzen. The singular value decomposition analysis was conducted by Stefan Franzen with input and assistance from Mst Sharmin Aktar. The writing of the manuscript was initially done by Mst Sharmin Aktar with guidance by Stefan Franzen and Reza Ghiladi.

Stefan Franzen wrote the final draft with advice from Reza Ghialdi, mainly editing by moving excess text to the Supporting Information for the sake of clarify. Funding was provided jointly by Stefan Franzen and Reza Ghiladi

#### **Declaration of Competing Interest**

The authors declare that they have no known competing financial interests or personal relationships that could have appeared to influence the work reported in this paper.

#### Data availability

Data will be made available on request.

### Acknowledgment

The authors gratefully acknowledge support from NSF grant CHE-2002954.

#### Appendix A. Supplementary data

Supplementary data to this article can be found online at https://doi.org/10.1016/j.jinorgbio.2023.112332.

### References

- [1] G. Yuan, M.A. Keane, Catal. Today 88 (1-2) (2003) 27-36.
- [2] R.E. Dodson, K.E. Boronow, H. Susmann, J.O. Udesky, K.M. Rodgers, D. Weller, M. Woudneh, J.G. Brody, R.A. Rudel, Int. J. Hyg. Environ. Health 230 (2020), 113624.
- [3] N. Hanif, T.A. Tyas, L. Hidayati, F.F. Dinelsa, D. Provita, N.R. Kinnary, F. M. Prasetiawan, G.A. Khalik, Z. Mubarok, D. Tohir, A. Setiawan, M. Farid, V. Kurnianda, A. Murni, N.J. Voogd De, Tanaka, Molecules 26 (21) (2021) 6328.
- [4] C.W. Act, F. Water, P. Control, A. Amendments, C.W. Act, Federal Water Pollution Control Act, U.S.C. 1251 et seq.. Generating Point Source., 2012, pp. 656–664.
   [5] N. Metal, C. Wastes, N. Metal, C. Wastes, Environmental Protection Agency 40 CFR
- Chapter 1, Appendix A 126 Priority pollutants Part 141 (1991) 663–664. 5.
- [6] E. Laurenti, E. Ghibaudi, S. Ardissone, R.P. Ferrari, J. Inorg. Biochem. 95 (2–3) (2003) 171–176.
- [7] M. Unger, L. Asplund, P. Haglund, A. Malmvarn, K. Arnoldsson, O. Gustafsson, Environ. Sci. Technol. 43 (21) (2009) 8245–8250.
- [8] L. Schmitt, I. Hinxlage, P.A. Cea, H. Gohlke, S. Wesselborg, Molecules 26 (21) (2021) 99.
- [9] Y.P. Chen, S.A. Woodin, D.E. Lincoln, C.R. Lovell, J. Biol. Chem. 271 (9) (1996) 4609–4612.
- [10] T. Malewschik, L.M. Carey, V. Serrano, R.A. Ghiladi, J. Inorg. Biochem. 236 (July) (2022), 111944.
- [11] J. Belyea, C.M. Belyea, S. Lappi, S. Franzen, Biochemistry. 45 (48) (2006) 14275–14284.
- [12] S. Franzen, M.P. Roach, Y.P. Chen, R.B. Dyer, W.H. Woodruff, J.H. Dawson, J. Am. Chem. Soc. 120 (19) (1998) 4658–4661.
- [13] R.E. Weber, C. Mangum, H. Steinman, C. Bonaventura, B. Sullivan, J. Bonaventura, Comp. Biochem. Physiol. Part A Physiol. 56 (2) (1977) 179–187.

- [14] J. Belyea, L.B. Gilvey, M.F. Davis, M. Godek, T.L. Sit, S.A. Lommel, S. Franzen, Biochemistry. 44 (48) (2005) 15637–15644.
- [15] A.H. McGuire, L.M. Carey, V. De Serrano, S. Dali, R.A. Ghiladi, Biochemistry 57 (30) (2018) 4455–4468.
- [16] N.L. McCombs, J. D'Antonio, D.A. Barrios, L.M. Carey, R.A. Ghiladi, Biochemistry 55 (17) (2016) 2465–2478.
- [17] D.A. Barrios, J. D'Antonio, N.L. McCombs, J. Zhao, S. Franzen, A.C. Schmidt, L. A. Sombers, R.A. Ghiladi, J. Am. Chem. Soc. 136 (22) (2014) 7914–7925.
- [18] M. Huan, M.K. Thompson, J. Gaff, S. Franzen, J. Phys. Chem. B 114 (43) (2010) 13823–13829.
- [19] V. De Serrano, J. Dantonio, S. Franzen, R.A. Ghiladi, Acta Crystallogr. Sect. D Biol. Crystallogr. 66 (5) (2010) 529–538.
- [20] K. Nienhaus, P. Deng, J. Belyea, S. Franzen, G.U. Nienhaus, J. Phys. Chem. B 110 (26) (2006) 13264–13276.
- [21] J. Dantonio, R.A. Ghiladi, Biochemistry 50 (27) (2011) 5999-6011.
- [22] R. Ten Have, S. Hartmans, P.J.M. Teunissen, J.A. Field, FEBS Lett. 422 (3) (1998) 391–394.
- [23] S. Franzen, K. Sasan, B.E. Sturgeon, B.J. Lyon, B.J. Battenburg, H. Gracz, R. Dumariah, R. Ghiladi, J. Phys. Chem. B 116 (5) (2012) 1666–1676.
- [24] International, M. B, A.S.K. Study, Pages 61–71 ADepartment of Chemistry, Moscow State University, 119899, Moscow, Russia; BDivision of Chemistry, G. V. Plekhanov Russian Economic Academy, Stremyanny Per. 28 45 (1) (1998) 61–71.
- [25] J. Feducia, R. Dumarieh, L.B.G. Gilvey, T. Smirnova, S. Franzen, R.A. Ghiladi, Biochemistry 48 (5) (2009) 995–1005.
- [26] T.L. Poulos, J. Kraut, J. Biol. Chem. 255 (17) (1980) 8199-8205.
- [27] Wabnitz, P. A.; Bowie, J. H.; Tyler, M. J.; Wallace, J. C.; Smith, B. P. 439 (1988) 1000 2844
- [28] M.A. Ator, S.K. David, P.R. Ortiz de Montellano, J. Biol. Chem. 262 (31) (1987) 14954–14960.
- [29] R.P. Ferrari, E. Laurenti, F. Trotta, J. Biol. Inorg. Chem. 4 (2) (1999) 232-237.
- [30] Q. Chang, J. Huang, Y. Ding, H. Tang, Molecules 21 (8) (2016).
- [31] S. Huang, Y. Qu, R. Li, J. Shen, L. Zhu, Microchim. Acta 162 (1-2) (2008) 261-268.
- [32] L.A. Dahili, I. Kelemen-Horváth, T. Feczkó, Process Biochem. 50 (11) (2015) 1835–1842.
- [33] J.A. Nicell, J.K. Bewtra, N. Bewas, C.C. St. Pierre, K.E. Taylor, Can. J. Civ. Eng. 20 (5) (1993) 725–735.
- [34] K. Kurnik, K. Treder, M. Skorupa-Klaput, A. Tretyn, J. Tyburski, Water Air Soil Pollut. 226 (2015) 8.
- [35] L.K. Folkes, L.P. Candeias, FEBS Lett. 412 (2) (1997) 305-308.
- [36] L.P. Candeias, L.K. Folkes, M. Porssa, J. Parrick, P. Wardman, Biochemistry 35 (1) (1996) 102–108.
- [37] L.P. Candeias, L.K. Folkes, P. Wardman, Biochemistry 36 (23) (1997) 7081–7085.
- [38] C.A. Sorrells, A.U. Shaikh, V.M. Samokyszyn, A. Shaikh, J. Ark. Acad. Sci. 56 (2002) 26.
- [39] P. Wardman, J. Phys. Chem. Ref. Data. 18 (4) (1989) 1637–1755.
- [40] M.F. Davis, H. Gracz, F.A.P. Vendeix, V. De Serrano, A. Somasundaram, S. M. Decatur, S. Franzen, Biochemistry 48 (10) (2009) 2164–2172.
- [41] L.M. Carey, R. Gavenko, D.A. Svistunenko, R.A. Ghiladi, Biochim. Biophys. Acta-Proteins Proteomics 1866 (2) (2018) 230–241.
- [42] L.M. Carey, K.B. Kim, N.L. McCombs, P. Swartz, C. Kim, R.A. Ghiladi, J. Biol. Inorg. Chem. 23 (2) (2018) 209–219.
- [43] Z. Otwinowski, W.P. Minor, Methods Enzymol. 276 (1997) (1993) 307–326.
  [44] V. De Serrano, Z. Chen, M.F. Davis, S. Franzen, Acta Crystallogr. Sect. D Biol.
- [44] V. De Serrano, Z. Chen, M.F. Davis, S. Franzen, Acta Crystallogr. Sect. D Biol Crystallogr. 63 (10) (2007) 1094–1101.

- [45] A.J. McCoy, R.W. Grosse-Kunstleve, P.D. Adams, M.D. Winn, L.C. Storoni, R. J. Read, Phaser crystallographic software, J. Appl. Crystallogr. 40 (4) (2007) 658–674
- [46] G.N. Murshudov, A.A. Vagin, E.J. Dodson, Acta Crystallogr. Sect. D Biol. Crystallogr. 53 (3) (1997) 240–255.
- [47] Project, C. C, The CCP4 suite: programs for protein crystallography, Acta Crystallogr. Sect. D Biol. Crystallogr. 50 (5) (1994) 760–763.
- [48] P. Emsley, B. Lohkamp, W.G. Scott, K. Cowtan, Acta Crystallogr. Sect. D Biol. Crystallogr. 66 (4) (2010) 486–501.
- [49] V.B. Chen, W.B. Arendall, J.J. Headd, D.A. Keedy, R.M. Immormino, G.J. Kapral, L. W. Murray, J.S. Richardson, D.C. Richardson, Acta Crystallogr. Sect. D Biol. Crystallogr. 66 (1) (2010) 12–21.
- [50] P. Le, J. Zhao, S. Franzen, Biochemistry 53 (44) (2014) 6863-6877.
- [51] C. Wang, L.L. Lovelace, S. Sun, J.H. Dawson, L. Lebioda, Biochemistry 52 (36) (2013) 6203–6210.
- [52] B.E. Sturgeon, B.J. Battenburg, B.J. Lyon, S. Franzen, Chem. Res. Toxicol. 24 (11) (2011) 1862–1868.
- [53] J. Zhao, V. De Serrano, J. Zhao, P. Le, S. Franzen, Biochemistry 52 (14) (2013) 2427–2439.
- [54] A.J. Barik, P.R. Gogate, Ultrason. Sonochem. 36 (2017) 517-526.
- [55] R.P. Hayes, T.W. Moural, K.M. Lewis, D. Onofrei, L. Xun, C. Kang, Int. J. Mol. Sci. 15 (11) (2014) 20736–20752.
- [56] A.H. McGuire, PhD. Dissertation. North Carolina State University, 2020.
- [57] J. Zhao, J. Moretto, P. Le, S. Franzen, J. Phys. Chem. B 119 (7) (2015) 2827–2838.
- [58] S. Franzen, L.B. Gilvey, J.L. Belyea, Biochim. Biophys. Acta Proteins Proteomics 1774 (1) (2007) 121–130.
- [59] S. Franzen, R.A. Ghiladi, L. Lebioda, J. Dawson, Chapter 10: multi-functional hemoglobin dehaloperoxidases, RSC Met. (4) (2016) 218–244.
- [60] V. De Serrano, S. Franzen, Peptide Sci. 98 (1) (2012) 27–35.
- [61] A.T. Smith, N.C. Veitch, Curr. Opin. Chem. Biol. 2 (2) (1998) 269-278.
- [62] N.K.D. Madhuresh, H. Nguyen, S. Franzen, J. Inorg. Biochem. 238 (2023) (2022), 112029.
- [63] J. D'Antonio, E.L. D'Antonio, M.K. Thompson, E.F. Bowden, S. Franzen, T. Smirnova, R.A. Ghiladi, Biochemistry 49 (31) (2010) 6600–6616.
- [64] S. Franzen, J. Belyea, L.B. Gilvey, M.F. Davis, C.E. Chaudhary, T.L. Sit, S. A. Lommel, Biochemistry 45 (30) (2006) 9085–9094.
- [65] J.B. Matthew, F.R.N. Gurd, Methods Enzymol. 130 (C) (1986) 413-436.
- [66] A. Henriksen, A.T. Smith, M. Gajhede, J. Biol. Chem. 274 (49) (1999) 35005–35011.
- [67] S.M. Khopde, K. Priyadarsini, I Biophys. Chem. 88 (1-3) (2000) 103-109.
- [68] M.K. Thompson, M.F. Davis, V. Serrano, F.P. Nicoletti, B.D. Howes, G. Smulevich, S. Franzen, Biophys. J. 99 (5) (2010) 1586–1595.
- [69] T. Malewschik, V. de Serrano, A.H. McGuire, R.A. Ghiladi, Arch. Biochem. Biophys. 673 (August) (2019), 108079.
- [70] T. Moreno-Chicano, A. Ebrahim, D. Axford, M.V. Appleby, J.H. Beale, A.K. Chaplin, H.M.E. Duyvesteyn, R.A. Ghiladi, S. Owada, D.A. Sherrell, R.W. Strange, H. Sugimoto, K. Tono, J.A.R. Worrall, R.L. Owen, M.A. Hough, IUCrJ 6 (2019) 1074–1085
- [71] L. Lad, M. Mewies, E.L. Raven, Biochemistry 41 (46) (2002) 13774–13781.
- [72] A. Gumiero, E.J. Murphy, C.L. Metcalfe, P.C.E. Moody, E.L. Raven, Arch. Biochem. Biophys. 500 (1) (2010) 13–20.
- [73] K.H. Sharp, P.C.E. Moody, K.A. Brown, E.L. Raven, Biochemistry 43 (27) (2004) 8644–8651.